

[Purchase  
Information](#)

[Information  
pour  
acheter](#)

[Titles  
Titres](#)

[←  
Article](#)

[→  
Article](#)



**Geological Survey  
of Canada**

**CURRENT RESEARCH  
2001-C18**

***Preliminary report on the geology and controlling  
parameters of the Goldcorp Inc. High Grade zone,  
Red Lake mine, Ontario***

***Benoît Dubé, Kenneth Williamson, and Michel Malo***



Natural Resources  
Canada

Ressources naturelles  
Canada

Canada

# CURRENT RESEARCH RECHERCHES EN COURS 2001

Purchase  
Information

Information  
pour  
acheter

Titles  
Titres

←  
Article

→  
Article



©Her Majesty the Queen in Right of Canada, 2001  
Catalogue No. M44-2001/C18E-IN  
ISBN 0-662-29861-6

Available in Canada from the  
Geological Survey of Canada Bookstore website at:  
<http://www.nrcan.gc.ca/gsc/bookstore> (Toll-free: 1-888-252-4301)

A copy of this publication is also available for reference by depository  
libraries across Canada through access to the Depository Services Program's  
website at <http://dsp-psd.pwgsc.gc.ca>

Price subject to change without notice

**All requests for permission to reproduce this work, in whole or in part, for purposes of commercial use, resale, or redistribution shall be addressed to: Earth Sciences Sector Information Division, Room 200, 601 Booth Street, Ottawa, Ontario K1A 0E8.**



## Preliminary report on the geology and controlling parameters of the Goldcorp Inc. High Grade zone, Red Lake mine, Ontario<sup>1</sup>

**Benoît Dubé, Kenneth Williamson, and Michel Malo<sup>2</sup>**  
GSC Quebec, Québec

Dubé, B., Williamson, K., and Malo, M., 2001: Preliminary report on the geology and controlling parameters of the Goldcorp Inc. High Grade zone, Red Lake mine, Ontario; Geological Survey of Canada, Current Research 2001-C18, 23 p.

<sup>1</sup> Contribution to Western Superior NATMAP Project

<sup>2</sup> INRS Géoressources,  
880 chemin Sainte-Foy,  
C.P. 7500, Sainte-Foy  
(Québec) G1V 4C7

### Abstract

*The association of axial planar carbonate veins, high-grade ore zones, and an  $F_2$  fold hinge deforming the basalt-ultramafic contact in the Goldcorp Inc. High Grade zone suggests a local geological control by an  $F_2$  fold. The development of such an  $F_2$  fold was potentially critical in forming the structures hosting the veins and in controlling fluid circulation allowing formation of the carbonate extensional veins within the basalt and their subsequent Au-rich silicic replacement. The  $CO_2$ -rich and auriferous silica-rich fluids were preferentially focused in a low-pressure  $F_2$  hinge due to a combination of factors including competence contrast, tangential longitudinal strain associated with  $F_2$ , and east-southeast-trending high-strain zones. The altered ultramafic rock acted as a less permeable barrier controlling fluid migration along the folded contact, allowing supralithostatic fluid pressure to build up and inducing a ponding effect in the basalt underneath, to create wide, high-grade ore zones in low-pressure hinges. The Au-rich silicic replacement of the carbonate veins was potentially syn- to late- $D_2$ . Subsequent strain remobilized gold in late, extremely high-grade structures.*



## Résumé

*L'association de veines carbonatées à plan axial, de zones minéralisées à forte teneur et d'une charnière de pli  $F_2$  qui déforme le contact basalte-roches ultramafiques dans la zone High Grade de la Goldcorp Inc. semble indiquer qu'un pli  $F_2$  a exercé un contrôle géologique local. La création d'un tel pli aurait été essentielle à la formation des structures hôtes des veines et au contrôle de la circulation des fluides qui a permis la formation de veines carbonatées de distension dans le basalte et leur remplacement par des fluides siliceux à forte teneur en or. Les fluides riches en  $CO_2$  et les fluides siliceux aurifères se sont concentrés préférentiellement dans une charnière  $F_2$  de basse pression suite à la venue de plusieurs facteurs, y compris un contraste de compétence, une déformation longitudinale tangentielle associée au pli  $F_2$  et la présence de zones fortement déformées à orientation est-sud-est. Les roches ultramafiques altérées ont agi comme une barrière moins perméable contrôlant la migration des fluides le long du contact plissé, permettant ainsi à la pression des fluides supralithostatiques de s'accroître et provoquant la formation d'un étang dans le basalte sous-jacent, créant ainsi de larges zones minéralisées à forte teneur dans les charnières de basse pression. Le remplacement des veines carbonatées par des fluides siliceux riches en or s'est vraisemblablement produit pendant ou vers la fin de la déformation  $D_2$ . Des déformations ultérieures ont remobilisé l'or dans des structures tardives à teneur extrêmement élevée.*

## INTRODUCTION

The world-class Campbell-Red Lake deposit being actively mined by Placer Dome Inc. (Campbell mine) and Goldcorp Inc. (Red Lake mine), is one of the largest and richest Canadian Archean gold deposits (>18 M oz Au (> 560 t)). It represents a very attractive style of mineralization due to its exceptionally high average grade (~21 g/t Au). The Goldcorp Inc. High Grade zone at the Red Lake mine has in reserves (proven and probable) 1 696 000 tons (1.538 Mt) at an average grade of 47 g/t Au (Goldcorp Inc.



1999 annual report) and constitutes an excellent example of such high-grade ore. Recent access to this zone presents a unique opportunity to better understand the fundamental geological parameters controlling its formation.

The Campbell-Red Lake deposit is a complex deposit and its genesis is still the subject of much debate. Penczak and Mason (1997) and Damer (1997) proposed a premetamorphic low-sulphidation epithermal origin whereas Andrews et al. (1986), Rogers (1992), Zhang et al. (1997), Tarnocai et al. (1998), and O'Dea (M. O'Dea, unpub. company report, 1999) concluded a synmetamorphic-syntectonic origin. A pre- to syn- to late deformational, multistage model was proposed by MacGeehan and Hodgson (1982). The deposit is hosted within a kilometre-scale heterogeneous strain corridor, informally known as the 'Red Lake mine trend'. The Campbell-Red Lake deposit potentially represents the end product of several stages of hydrothermal alteration and increments of brittle-ductile deformation (cf. MacGeehan and Hodgson, 1982).

In the summer of 2000, we mapped in detail the 34th level as well as some other key localities in the 30th and 32nd levels of the High Grade zone as part of the Western Superior NATMAP Project. The objectives of our long-term study are 1) to define the geological characteristics and setting of the High Grade zone with emphasis on the structures and paragenetic sequence of alteration, vein, and mineralization in order to understand why the grade is so high; and 2) to better understand the processes responsible for the formation of the High Grade zone in relationship with other ore types and hydrothermal events as well as defining the evolution of hydrothermal fluids through time.



## REGIONAL GEOLOGICAL SETTING

The Red Lake greenstone belt is dominated by Mesoarchean rocks including the volcanic-dominated Balmer (2.99 Ga), Ball (2.94–2.92 Ga), and Bruce Channel (2.894 Ga) assemblages. These Mesoarchean rocks were tilted by a pre- $D_1$  episode of deformation (Sanborn-Barrie et al., 2001). An angular unconformity separates Mesoarchean rocks from the Neoproterozoic volcanic rocks of the ca. 2.75–2.73 Ga Confederation assemblage. The unconformity is defined by polymictic conglomerate located at the interface between Mesoarchean and Neoproterozoic strata, and indicates that the main stages of crustal growth from ca. 3 Ga to 2.7 Ga were primarily depositional, not tectonic (Sanborn-Barrie et al., 2000).

Evidence of two main episodes of deformation ( $D_1$ ,  $D_2$ ) imposed after ca. 2.742 Ga volcanism is widespread (Sanborn-Barrie et al., 2001). The main stages of penetrative deformation resulted in two sets of folds ( $F_1$  and  $F_2$ ). A locally recognized northerly trending  $S_1$  foliation is associated with  $F_1$  folds, whereas widespread, weakly to moderately developed,  $S_2$ - $L_2$  fabric is associated with  $F_2$  folds which trend east to northeasterly.  $D_2$  is contemporaneous to the emplacement of the 2.718 Ga Dome Stock (Sanborn-Barrie et al., 2001). Deviation in the orientation of interpreted  $S_2$  from the regional (east- to northeast-striking)  $D_2$  trend, to an east-southeasterly striking protracted heterogeneous strain corridor ('Red Lake mine trend') between Cochenour and Balmertown may be associated with a change in local boundary conditions in the eastern Red Lake belt during  $D_2$  (Sanborn-Barrie et al., 2001). Localization of strain into a belt-scale system of conjugate shear zones (cf. Andrews et al., 1986) is not supported by recent studies (Sanborn-Barrie et al., 2001). The majority of gold deposits in the Red Lake district are proximal to a regional angular unconformity between the ca. 2.99 Ga Balmer and ca. 2.74 Ga Confederation assemblages. The major gold deposits represent the end-product of hydrothermal replacement and constitutes atypical greenstone-hosted gold types.



## LOCAL GEOLOGICAL SETTING

The Campbell-Red Lake gold deposit is hosted by the tholeiitic to komatiitic rocks of the Balmer assemblage. In the vicinity of the deposit, the lithological sequence consists predominantly of basalt and ultramafic rocks with subordinate rhyolite, diorite, and synvolcanic sedimentary rocks (Penczak and Mason, 1997)(**Fig. 1A**). These rocks have been folded by southeast-trending  $F_2$  folds which are transected by two steeply dipping ( $70^\circ$ – $80^\circ$ S), southeast-trending subparallel faults, the Campbell and Dickenson faults. The geometry of rock units at the Red Lake mine is characterized by alternating southeast-trending  $F_2$  antiforms-synforms, in which the northeast pair of folds are transected by the southwest-dipping Dickenson Fault (Fig. 1). Based on the apparent displacement of lithologies along these faults, the Campbell Fault was interpreted as a sinistral strike-slip fault, whereas the Dickenson Fault is a dextral strike-slip fault (Mathieson, 1982; Penczak and Mason, 1997); however, the geometry of carbonate veins in the G and L zones of the Campbell mine are compatible with a dextral component of motion along the Campbell Fault. More recently, O'Dea (M. O'Dea, unpub. company report, 1999) proposed that both faults are part of an imbricated reverse-sinistral fault system developed along the limbs of a pre-existing isoclinal  $F_2$  antiform as a result of a progressive change in strain accommodation.

The High Grade zone, currently exploited on levels 32 and 34 in the Red Lake mine, is located up to 150 m in the hanging wall of the East South 'C' ore zone. The East South 'C' ore zone, on level 34, corresponds to a strongly foliated sulphide-rich (pyrrhotite-pyrite-arsenopyrite-magnetite) replacement zone hosted within the Dickenson fault zone. The High Grade zone is essentially hosted by basalt and occurs within an  $F_2$  antiform defined by the geometry of the rhyolite to the west and the basalt-ultramafic rock contact to the southeast of the High Grade zone (**Fig. 1B**). Both fold limbs are strongly attenuated by  $S_2$ ,



particularly towards the Dickenson Fault to the northeast. The  $F_2$  fold is responsible for the apparent thickening of the basalt in the hinge zone. This fold is affected by parasitic subparallel folds, and a complex 'M' pattern in the hinge zone.

The basalt is aphanitic and massive. It occasionally contains flattened amygdales and varioles (see **Fig. 4A**). Two distinct ultramafic rocks are recognized, basaltic komatiite and peridotitic komatiite.

All these units are cut by quartz-feldspar and feldspar porphyritic rocks and lamprophyre dykes (**Fig. 1B, 2, 3**). The quartz-feldspar porphyry and feldspar porphyry dykes are northwest to east to east-southeast trending and the feldspar porphyry cuts high-grade ore zones on levels 32 and 34. In the 32-826-8W stope on level 32 (**Fig. 3B**), a feldspar porphyry of this type, cutting through the ore, is moderately foliated (N140/55°), suggesting that it was submitted to, at least, the last increments of the  $D_2$  deformation. The age of this dyke will be determined by U-Pb geochronology.

Three sets of lamprophyre dykes are present. One set is subparallel to the regional  $S_2$  fabric (N130/70°), a second set strikes south with a shallow dip to the west, and a third set is east trending and steeply dipping. These lamprophyre dykes cut the High Grade zone (**Fig. 3A**).

## STRUCTURE

Rocks in the High Grade zone area were folded and sheared by the main  $D_2$  regional deformation episode. No evidence of  $D_1$  structures was observed in the study area. Figure 1B illustrates that in the High Grade zone, the ultramafic rocks, basalt, and rhyolite are folded by an east-southeast-trending  $F_2$  antiform, moderately plunging to the east-southeast (55°).  $F_1$  folds, refolded by  $F_2$  are present in the Confederation sediments exposed at surface (MacGeehan and Hodgson, 1982; M. O'Dea, unpub.





company report, 1999; Sanborn-Barrie et al. 2001) and most probably have an influence on the distribution of the units in the mine. Such refolded folds can explain the opposite structural facing between the steep to moderate westerly plunge of the  $F_2$  folds in the Campbell mine and the moderate east-southeast plunge in the Red Lake mine.

In the hinge zone of the  $F_2$  antiform, a weakly developed, axial planar east-southeast-trending and southwest-dipping (mean:  $N127/63^\circ$ )  $S_2$  foliation represents the main fabric developed in the basalt. Although the deformation is heterogeneous, the overall strain in the hinge zone is low to moderate; however,  $S_2$  is locally more intense, defining local centimetre- to metre-wide, east-southeast-trending high-strain zones, which coincide to high-grade mineralization and alteration.  $S_2$  locally contains a  $L_2$  stretching lineation with a moderate plunge to the west (mean:  $N269/50^\circ$ ), defined by elongate quartz-carbonate-filled amygdales in basalt with aspect ratio of 3:1 or less. Both limbs of the  $F_2$  antiform are transposed by ductile shear zones, known as the footwall and hanging wall shears (**Fig. 1B, 2**). The footwall shear is a 5 m wide high-strain zone. It can be traced laterally for up to 300 m and does not appear to contain gold mineralization. The footwall shear is characterized by an intense  $S_2$  foliation, striking  $N135/58^\circ$  and contains abundant foliation-parallel carbonate veins. Asymmetric boudins deforming one of these carbonate veins suggest a reverse component of motion.

The hanging wall shear zone transects the southern limb of the  $F_2$  antiform. This southeast-trending and moderately southwest-dipping ( $\sim N133/61^\circ$ ) shear zone can be traced for over 500 m along strike (**Fig. 1B, 2**). The hanging wall shear is more than 10 m wide and is characterized by a penetrative  $S_2$  fabric deforming the host basalt and decimetre-wide arsenopyrite- and biotite-rich bands as well as millimetre- to centimetre-wide foliation parallel carbonate veins (**Fig. 4B**). Locally, west-plunging  $L_2$  mineral lineations ( $\sim N269/50^\circ$ ) on  $S_2$  (**Fig. 4C**) are colinear to a minor asymmetric  $F_2$  fold axis deforming the carbonate vein.



Two other sets of smaller high-strain zones are present to the southwest of the hanging wall shear. An east-west, steeply south-dipping high-strain zone known as the east-west shear (**Fig. 2**), averages 3–4 m wide and is characterized by a well developed foliation trending N105/75°. As for the hanging wall shear, this foliation is particularly developed in biotite-arsenopyrite-sericite-rich alteration zones hosting subparallel and locally oblique silicified carbonate veins. This structure can be traced over 100 m to the west, whereas its eastern termination merges with the hanging wall shear. This east-west high-strain zone cuts a south-southeast-trending high-strain zone (zone HW5), as demonstrated by an apparent dextral offset (Fig. 2).

The HW5 high-strain zone is moderately dipping to the west (~N160/48°) and is defined as biotite- and/or arsenopyrite-rich zones. It also contains sheeted carbonate veins, up to 60 cm wide, subparallel to the enclosing south-southeast-trending fabric; some are also at a high angle and crenulated.

The east-southeast-trending  $S_2$  fabric and parallel carbonate veins represent the main structure. North-northwest-trending carbonate veins and their silicified gold-bearing equivalents are crenulated by the east-southeast  $S_2$  fabric and are cut by the east-southeast-trending vein and magnetite-pyrrhotite-pyrite-arsenopyrite replacement ore zones of the hanging wall shear. All these east-southeast-, east-, and south-southeast-trending structures (footwall, hanging wall, east-west, and HW5) intersect each other at approximately N275/45°. This intersection axis is almost colinear to the  $L_2$  lineation and to the fold axis deforming the veins (Fig. 2B–E).

Gold-bearing metre-wide east-west shear zones (090/65°) are locally developed in the ultramafic rocks close to and parallel to the basalt contact. Carbonate breccia bodies contain flattened fragments of intensely carbonatized wall rock indicating that the east-west shear is clearly late in the breccia formation process or postdates it. West-southwest-plunging striations (254/28°) with steps are developed on shear planes and indicate an oblique sinistral-reverse sense of motion.



The various sets of carbonate veins developed within the high-strain zones or hosted by centimetre- to metre-scale  $S_2$  foliated zones within the lower strain  $F_2$  hinge, were deformed. They were submitted to asymmetric boudinage with antithetically rotated asymmetric pull-aparts or back rotated layer segments (Hanmer and Passchier, 1991; Jordan, 1991) enclosed in foliated ( $S_2$ ) basalt (**Fig. 4D–E**). Although such kinematic indicators should be used with caution as they are ambiguous kinematic indicators, these asymmetric boudins suggest a reverse-sinistral sense of motion. The shear fracture ( $S_c$ ) isolating each segment are subhorizontal to shallow, southwest to northwest dipping, and are commonly filled by amphibole suggesting that deformation probably occurred at amphibolite grade. The elongation axis of the boudins is oriented at about  $N270/50^\circ$ , parallel to  $L_2$ . Locally, subparallel asymmetric boudins deforming carbonate veinlets are confined within wall-rock fragments hosted by large north-northwest-trending carbonate breccia veins. This indicates that the veins within the fragments were deformed after formation of the breccia vein. Depending of their original orientation, the carbonate veins are also commonly folded by Z-shape, small-scale  $F_2$  folds consistent with a reverse component of motion.

The contact between the late lamprophyre and the host basalt is locally affected by brittle faults and marked by striations with a shallow to moderate plunge to the northwest. These striations are oriented  $155/35^\circ$  and show well developed steps indicating a sinistral-normal motion which is also supported by apparent sinistral offset of feldspar porphyry dykes by crosscutting, steeply dipping lamprophyre. Some walls of silicified carbonate veins are also marked by a brittle fault plane with shallow westerly plunging striations ( $277/06^\circ$ ) (e.g. 34-786-4W stope).



## CARBONATE VEINS

Carbonate veins (Fe-dolomite-siderite-ankerite) are very abundant and illustrate the large-scale CO<sub>2</sub>-rich hydrothermal fluid circulation characterizing the entire Campbell-Red Lake deposit area (e.g. Parker, 2000). These veins are commonly barren or contain low-grade mineralization associated with sphalerite (e.g. Penczak and Mason, 1997). They are extensively developed in the basalt but are also present in the rhyolite and ultramafic rocks. In the High Grade zone, three sets of barren carbonate sheeted veins hosted by basalt can be distinguished based on their internal texture and/or orientation. They are parallel to the three types of ore described by Rogers (1992). The first set, and by far the most common, corresponds to east-southeast-trending and moderately southwest-dipping (N129/63°) carbonate veins with well developed colloform-crustiform banding and local breccia (**Fig. 2C**). These veins are hosted by a few centimetres- to tens of metres-wide zones of foliated (S<sub>2</sub>) basalt. The veins are commonly subparallel to the S<sub>2</sub> foliation and are axial planar to the F<sub>2</sub> fold (**Fig. 2**).

The second set of veins is less abundant and correspond to colloform-crustiform veins very similar to the first set, but strike N167/56°, subparallel to an enclosing foliation (**Fig. 2A–C**). This set is commonly cut by the main east-southeast-trending set. The thickness of these sets of veins varies from a few millimetres to a few metres. The smaller veins are relatively massive whereas crustiform-colloform texture with symmetric millimetre-wide bands are present in the thicker veins. Both sets of veins locally contain carbonate fibres perpendicular to banding and/or vein walls.

The third set of veins corresponds to large carbonate breccia veins (**Fig. 4F**) oblique to the S<sub>2</sub> fabric and associated with east-southeast-trending colloform extension vein arrays of the first set. These foliation-oblique breccia veins are usually north-northwest trending and moderately west dipping (N166/43°). They are subparallel to the second vein set, but have a slightly shallower dip. The breccia veins are up to 8–10 m wide and can be traced for several tens of metres along strike. Internally, the breccia veins show



complex textures with centimetre- to metre-long angular wall-rock fragments, colloform-crustiform banding, cockade texture (**Fig. 4F–G**), and earlier vein fragments. Jigsaw puzzle breccia are common and rock bridges are locally present. Several smaller, subparallel sheeted veins with colloform texture flank the larger breccia vein. Some of the rock fragments contain flattened varioles, defining a foliation striking N130/50° subparallel to  $S_2$ . Other rock fragments are cut by carbonate veinlets, striking N125/70°. Such a large north-northwest-trending breccia vein, with adjacent extension vein arrays, is present on level 34 and is located between two east-southeast-trending well foliated zone ( $S_2$ ) and foliation-parallel east-southeast carbonate veins (**Fig. 2**). This geometrical relationship suggests that the large north-northwest-trending breccia vein represents a dextral dilational jog accommodating displacement along the east-southeast  $D_2$  structures. These carbonate breccia veins are commonly barren although significant mineralization is present as pipe-like silicified zones at the intersection with the east-southeast veins. Locally, silicified and biotitized mineralized wall-rock fragments with pyrrhotite and pyrite are hosted by the barren breccia. This indicates that, at this locality, part of the mineralization predates or was early in the carbonate veining process and illustrates the long hydrothermal history of the deposit (see *also* M. O’Dea, unpub. company report, 1999). Locally, wall-rock fragments present in the north-northwest-trending breccia are foliated but this foliation is parallel from one fragment to the other and is subparallel to the  $S_2$  fabric present outside the veins, suggesting that ductile deformation outlasted the breccia development.

Spectacular barren carbonate stockwork and breccia units are hosted by strongly carbonatized and silicified green mica-biotite-rich ultramafic rocks close to the folded contact with the basalt. These stockwork zones contain up to 30–40% of unoriented to sheeted carbonate veins and breccia. The stockworks are locally cut by east-southeast-trending carbonate veinlets parallel to the first set.



## LATE QUARTZ VEINS

Late north-trending and shallow-dipping (000/45–350/35°) quartz veins are locally present. These veins are barren and mostly confined within late lamprophyre dykes. They are essentially composed of euhedral quartz crystals perpendicular to the vein walls indicating that they represent extensional veins compatible with  $L_2$ .

## GOLD MINERALIZATION AND ASSOCIATED ALTERATION

The High Grade zone is characterized by multi-ounce ore zones located within or near the  $F_2$  hinge area and essentially hosted by the basalt (**Fig.1B, 2**). These ore zones have a known lateral extent of about 130 m and were formed by selective silicic replacement of a vast number of the three sets of carbonate colloform-crustiform and breccia veins and of enclosing wall-rock selvages (**Fig. 4H**). This silicic replacement is associated with variable amounts of fine arsenopyrite (0–30%), and trace amount to 3–5% fine pyrite and/or pyrrhotite and rare brown-red and yellow sphalerite. The replacement zones also commonly contain altered wall-rock clasts replaced by arsenopyrite, biotite, and/or quartz-sericite. The intensity of the silicic replacement is highly variable. It is common to see that the silicification and associated pyrite and/or arsenopyrite only occur along the margins of the carbonate veins as glassy replacement quartz with or without arsenopyrite-rich selvages. Significant high-grade mineralization is also located at the silicified intersection between the north-northwest-trending carbonate breccia veins and the east-southeast-trending carbonate veins and structures. Locally, the High Grade zone is hosted by shallow-dipping and folded ( $F_2$ ) arsenopyrite-rich silicified carbonate veins, as well as quartz veins (**Fig. 5A**) with 5–6% pyrite, pyrrhotite, and fine arsenopyrite.



The hanging wall shear is one of the main gold-bearing structures of the High Grade zone. It hosts significant high-grade gold mineralization in the  $F_2$  hinge area but the grade significantly diminishes along strike towards the northwest. In the hanging wall shear, a significant portion of the high-grade ore zones consist of grey sulphide-rich disseminated replacement and breccia zones within altered basalt hosting silicified carbonate veins. The ore mineralogy varies from predominately arsenopyrite to pyrrhotite-pyrite-arsenopyrite-magnetite-rich assemblages or magnetite-rich assemblages. Where heavily mineralized, the hanging wall shear occurs as a laminated, dark, magnetite-rich silicified replacement zones. These ore zones also contain abundant biotite and 3–5% pyrite as disseminations and foliation-parallel veinlets occurring with numerous carbonate veinlets transposed by  $S_2$  and partly or totally replaced by fine-grained quartz (**Fig. 4B**). The high-grade ore is also associated with strongly foliated semimassive arsenopyrite-rich bands and/or layers up to 40 cm wide.

In the High Grade zone, the wall-rock alteration developed in the host basalt adjacent to silicified carbonate vein is of limited extent and characterized by centimetre- to metre-wide alteration halos. Two stages of alteration are present, an outer metre-wide garnet-magnetite-chlorite-amphibole-aluminous alteration (e.g. Damer, 1997) and a centimetre-wide proximal biotite-iron carbonate replacement zone associated with variable amount of arsenopyrite (0–35%), pyrite, pyrrhotite, and magnetite (0–12%) (Fig. 4B). The latter zone is symmetrically distributed in the heterogeneously foliated basalt hosting the veins. In the High Grade zone, biotite-carbonate-rich alteration is commonly replaced by inner sericite-quartz±actinolite alteration directly associated with mineralization. In the outer zone, garnet forms euhedral to elongated crystals representing 25–35% of the host basalt mineralogy. They are elongated parallel to the  $S_2$  foliation. In the ultramafic rocks, the alteration is typified by abundant iron-carbonate with green mica minerals.



Visible gold is very common in the carbonate veins replaced by glassy quartz (**Fig. 5D–G**) and is associated with traces of very fine-grained pyrite and arsenopyrite. Visible gold also coats late shallow-dipping fractures and striated fault planes at high angle to the main  $S_2$  fabric (**Fig. 5B**). Extreme high-grade samples show gold as fracture fillings at high angle to the main  $S_2$  fabric and as replacement of small carbonate veinlets cutting across foliated magnetite-biotite-rich basalt in the vicinity of the hanging wall shear (**Fig. 5C–D**). Locally, gold is present in fractures filling the axial planar cleavage of  $F_2$  folds deforming silicified north-northwest-trending carbonate veins.

## TIMING OF GOLD DEPOSITION

The timing of the gold-rich silicic replacement of the carbonate vein relative to  $D_2$  deformation is a critical element in the understanding of the formation of the High Grade zone. In the East South 'C' ore zone (16th level, 16-01-7 stope), sulphidic wall-rock replacement mineralization is cut by barren carbonate breccia veins. In the High Grade zone, silicic arsenopyrite-rich mineralization overprinting pre-existing colloform-cockade carbonate breccia is, in turn, brecciated by arsenopyrite-rich mineralization. These stages of arsenopyrite mineralization are themselves cut by colloform-banded carbonate-quartz veinlets and breccia containing arsenopyrite and visible gold. These relationships clearly illustrate multiple stages of gold deposition, silicic replacement, and carbonate veining; however, there is indication, in the High Grade zone (34th level), that the timing of the gold-bearing silicic event is potentially associated with a deformation event superimposed on the barren carbonate vein. In one location, carbonate veinlets have been strongly replaced by Au-rich quartz, but preserved shallow-dipping amphibole is hosted in a fine-grained quartz matrix with local remnants of asymmetric boudins of carbonate vein (**Fig. 4D, 5E–F**). This suggests that the replacement and gold deposition could have been at the same time as or after the development of the asymmetric boudins. In another location, Au-rich quartz replaces a





carbonate vein and infills the space between the lozenge-shaped asymmetric boudins. Both the carbonate and the replacing Au-rich quartz are cut by a shear plane (**Fig. 5G–H**). These relationships have been only locally observed and will definitely require further investigation. If confirmed by petrographical studies, this will suggest that at least part of the gold-bearing silicic replacement of the carbonate vein in the High Grade zone is syn- $D_2$  to late  $D_2$ . Alternatively, some high-grade silicified carbonate veins hosted by the southeast- and south-southeast-trending high-strain zones are at high angle to, and crenulated-folded by  $F_2$  (**Fig. 5A**). This indicates that such high-grade gold mineralization has accommodated a large part of the  $D_2$  deformation and is early  $D_2$  or pre- $D_2$ . More work is definitely needed to better define the timing of gold deposition.

## DISCUSSION

The Campbell-Red Lake deposit shares analogies with low-sulphidation epithermal gold deposits, including the colloform-crustiform-cockade texture of the carbonate veins, the Au-As-Sb-Zn-Hg metallic signature, aluminous alteration, and the silicic replacement of the carbonate veins (e.g. Penczak and Mason, 1997); however, the timing of the gold-rich silicic emplacement relative to magmatism, deformation, metamorphism, and carbonate veining remains controversial (Penczak and Mason, 1997; Zhang et al., 1997; Tarnocai et al., 1998; M. O’Dea, unpub. company report, 1999; Parker, 2000). Recently, O’Dea (M. O’Dea, unpub. company report, 1999) proposed a syn- $D_2$  shear-related model where the colloform carbonate veins hosting the ore corresponds to highly deformed extensional veins originally formed perpendicular to west-plunging  $L_2$  lineations.

The Campbell-Red Lake deposit definitively shows a spatial relationship between mineralization and the Campbell and Dickenson faults (**Fig. 1**). The cymoid loop and horsetail geometry of ore zones like the L-zone at Campbell mine, and the location of a large number of ore zones within the Dickenson Fault



indicate that these faults have played a fundamental role in the formation of the deposit by controlling vein geometry and fluid access (e.g. Penczak and Mason, 1997 and references therein); however, the timing of these faults and their structural evolution remain controversial. Furthermore, the ore zones are commonly deformed by foliation and folding and have clearly recorded part of the  $D_2$  strain. Do these large faults represent early strike-slip structures, controlling the formation of the vein field and mineralization? Were they formed at upper level in the crust and then buried and deformed by  $D_2$  ductile deformation as proposed by MacGeehan and Hodgson (1982) and Penczak and Mason (1997)? The common occurrence of  $F_2$  folds deforming the carbonate veins would be compatible with such an interpretation. Alternatively, do these faults represent the end product of a protracted  $D_2$  event that included fold tightening and transposition of the limbs (e.g. Zhang et al., 1997; M. O'Dea, unpub. company report, 1999)?

At a larger scale, there is also an empirical relationship between high-grade ore hosted by Au-rich silicified colloform carbonate veins and the basalt-ultramafic contact (e.g. Rigg and Helmsteadt, 1981). The veins are commonly oriented at a high angle to, and close to that contact and the density and thickness of high-angle extensional veins decrease away from this contact. Beside primary permeability, especially in the basaltic komatiite, the competence contrast between the basalt and ultramafic rocks and the high-angle relationship between this contact and the Campbell and Dickenson strain corridor (mine trend) and associated structures, have largely controlled the fracture pattern and fluid access. A major part of the Au-rich hydrothermal fluids were channelled along the basalt-ultramafic contact; however, what controls the high angle relationship between the basalt-ultramafic contact and the host structures?

In the High Grade zone, most of the carbonate veins share some analogies with fault-fill veins as shown by their banded structure and their orientation subparallel to the  $S_2$  foliation developed in their host basalt; however, the pristine colloform-crustiform and cockade internal textures of the three sets of carbonate vein breccia zones with carbonate fibres at high angle to vein walls indicate that they are open-space-filling extensional veins. As such, they are structurally incompatible with the adjacent



subparallel foliation as originally recognized by MacGeehan and Hodgson (1982) elsewhere in the deposit. Furthermore, these extensional veins and/or breccia zones are not compatible with the  $L_2$  stretching lineations as they are not perpendicular to it. The veins and/or breccia zones are west dipping whereas they should be east dipping to be compatible with  $L_2$  (Fig. 2B–C). Therefore, there is a structural incompatibility between these carbonate veins and the host  $S_2$  structures. It is possible that the three sets of veins are filling fractures formed pre- $D_2$  (? $D_1$ ) to early- $D_2$  at the initiation of the  $F_2$  folds in response to northeast-southwest shortening. The location of the three sets of silicified carbonate veins in, or near, the hinge of the  $F_2$  fold and the high-angle relationship between veins and the folded ultramafic-basalt contact suggest that they may represent extensional fissures formed in the outer arc of the  $F_2$  antiform due to tangential longitudinal strain (Ramsay and Huber, 1987) (Fig. 6). The relatively higher competence of the basalt compared to the ultramafic rock (basaltic komatiite), before carbonatization, suggests that in the outer arc of the  $F_2$  hinge, the basalt would be submitted to layer-parallel stretching allowing development of extensional fissures at high angle to the folded contact (Fig. 6B–D). The extensional fissures being syn- $F_2$  fold and infilled by  $CO_2$ -rich fluid. Layer-parallel foliation and veins could have developed along the contact between the two contrasting units to accommodate the strain. The model also predicts possible development of conjugate shear faults in the outer arc of the competent unit (Fig. 6C). As the strain continues to be accommodated and the shortening of the units, increases due to tightening of the fold, the  $S_2$  axial planar foliation continues to develop, local centimetre- to metre-wide high-strain zones are formed and superimposed on the already developed extensional carbonate veins. This will imply that the fold evolved from a concentric-parallel fold (Fig. 6) to a similar fold (Fig. 1B) due to subsequent flattening during  $D_2$ . Ultimately, the limbs of the  $F_2$  folds were strongly attenuated and transposed within  $D_2$  high-strain zones to produce larger ductile structures such as the footwall and hanging wall shear zones on both sides of the hinge zone. In such a model, the Dickenson fault zone coincides with strongly transposed fold limbs as suggested by O’Dea (M. O’Dea, unpub. company report, 1999).



This preliminary model may explain the extensional nature of the carbonate veins, the subparallel  $S_2$ , and the subsequent flattening and deformation of these veins by reverse-sinistral asymmetric boudins and asymmetric  $F_2$  folds. It also explains why a vast number of ore zones at the Campbell-Red Lake deposit are at high angle to the folded basalt-ultramafic contacts and mostly confined within basalt. Layer-parallel flexural slip along the northeast limb of the  $F_2$  antiform is consistent with formation of a dextral dilational jog geometry, illustrated by the north-northwest-trending breccia vein (third set), linking two east-southeast-oriented auriferous higher strain segments. Such a dilational jog is also compatible with the dextral component of motion along the Dickenson Fault. The east- and south-southeast-foliated zones hosting the veins are conjugate sets of shears compatible with deformation induced by tangential longitudinal strain in the outer arc of the fold and their intersection define west-plunging ore shoots (**Fig. 2E, 6C**); however, these zones could also represent conjugate oblique-slip zones related to progressive shortening perpendicular to the east-southeast-trending main fabric as proposed at Campbell mine by Zhang et al. (1997) .

More importantly, the model would explain the spatial relationship between auriferous silicified colloform-crustiform carbonate veins and breccia zones with  $F_2$  hinges, the early timing of these carbonate veins relative to  $D_2$ , and their subsequent deformation. The  $F_2$  fold-related model will predict development of a fanning pattern of extensional fractures in the hinge zone of the  $F_2$  folds (**Fig. 6**). This fanning pattern is not clearly observed in the High Grade zone. Steeply dipping north-northeast-trending colloform carbonate veins in East South 'C' ore zone are crenulated by and at high angle to  $S_2$  (Mathieson and Hodgson, 1984; Rogers, 1992). They could represent extensional veins compatible with such a fanning pattern.



Another important aspect in the geometric and possible genetic controls of the  $F_2$  fold on the formation of the High Grade zone is that the gold-bearing silicic replacement of the carbonate veins has occurred essentially in the fold hinge of the  $F_2$  antiform and over 130 m from the folded basalt-ultramafic contact (Fig. 1, 2). The auriferous silica-rich fluid was focused in the low-pressure  $F_2$  hinge zone. The ultramafic rocks are structurally above the basalt and may have acted mechanically and chemically as a less permeable barrier controlling fluid migration along the contact as proposed by MacGeehan and Hodgson (1982) for the 2151 W zone at Campbell mine. Such a barrier could allow supralithostatic fluid pressure to build up to form the large carbonate stockwork veins and associated carbonatization in the ultramafic rocks at the contact with the basalt, sealing the ultramafic rocks and inducing a ponding effect in the basalt underneath to create the high-grade ore. The hinge acted as a low-pressure zone where high fluid flow was preferentially channellized. There, the gold-rich silicic fluid has replaced the carbonate vein and infilled any permeable zones including the high-grade hanging wall shear. The latter has acted as a feeder zone focusing extremely Au-rich fluid within and around the hanging wall shear.

An  $F_2$  fold-related model would explain the abundance of carbonate colloform veins near, and their gradual decrease in abundance and thickness away from, the basalt-ultramafic hinge zones. It also explains why the best grade of ore in the entire Campbell-Red Lake mine is hosted in or near  $F_2$  hinges (M. Chownainec, pers. comm., 2000). Late  $D_2$  to post- $D_2$  strain has partially remobilized gold in late fractures in the  $F_2$  hinge zone area and produces extremely rich zones.

At a much smaller scale, if petrographical study confirms that the asymmetric boudins deforming the carbonate veins predate the gold-rich silicic replacement or were synchronous, this will become a key geological element to help define the chronology between the  $CO_2$ -rich fluid, the auriferous silicic replacement, and the heterogeneous  $D_2$  protracted deformation. An ongoing U-Pb geochronological program on foliated altered dykes and foliated porphyry dykes that postdated ore deposition will be a key in helping to define the chronology of events.



## CONCLUSIONS

The Campbell and Dickenson faults have played a fundamental role in the formation of the Campbell-Red Lake deposit by controlling vein geometry and fluid access. In the High Grade zone, the empirical relationships between abundance and thickness of carbonate veins, high-grade ore zones, and  $F_2$  fold hinge deforming the basalt-ultramafic contact suggest a possible geological control by the  $F_2$  fold on its formation. Our current working hypothesis proposes that the auriferous silica-rich fluid was focused into  $F_2$  hinge zones due to a combination of factors including competency contrast between the basalt and ultramafic rocks, tangential longitudinal strain associated with the  $F_2$  folding, and east-southeast high-strain zones associated with fold tightening and transposition. The strongly altered and veined ultramafic rocks have acted as a mechanically less permeable barrier controlling fluid migration along the contact, allowing supralithostatic fluid pressure to build up, and inducing a ponding effect in the basalt underneath to create wide high-grade ore in the  $F_2$  hinge. Such a structural trap represents the best exploration target for High Grade zone style mineralization.

The carbonate veins represent a first hydrothermal 'ground preparation' stage for the following, and syn- $D_2$  to late  $D_2$ , Au-rich silicic replacement. Subsequent strain remobilized gold in late, extremely high-grade structures.

The combination of multiple hydrothermal events, several strain increments with gold deposited and remobilized in the low-pressure hinge zones of the  $F_2$  fold, could be responsible for the exceptionally rich ore of the High Grade zone. One important exploration implication for the district is that the amphibolite rocks can be prospective for high-grade gold mineralization.



## ACKNOWLEDGMENTS

Goldcorp Inc. in particular Gilles Fillion, Stephen McGibbon, Rob Penczak, Tim Twomey, Mark Epp, Michael Dehn, and the production staff at the Red Lake mine, are thanked for their scientific collaboration, logistical, and financial support, critical review, and permission to publish. Mary Sanborn-Barrie, Tom Skulski, and John Percival of the GSC as well as Jack Parker and Carmen Storey of the Ontario Geological Survey are thanked for their collaboration and numerous constructive discussions in the field. Placer Dome Inc., in particular S. Morris, R. Dutka, M. Mytny, M. Chownainec, and C. Tarnocai, are sincerely thanked for underground visits at the Campbell mine and for sharing their knowledge. Critical reviews by Kathleen Lauzière and Alain Tremblay helped improved the manuscript.

## REFERENCES

**Andrews, A.J., Hugon, H., Durocher, M., Corfu, F., and Lavigne, M.**

1986: The anatomy of a gold-bearing greenstone belt: Red Lake, northwestern Ontario; *in* Gold '86 Symposium; Gold'86, Toronto, Ontario, September 28–October 1, 1986, p.

**Damer, G.C.**

1997: Metamorphism of hydrothermal alteration at the Red Lake Mine, Balmertown, Ontario; M.Sc. thesis, Queen's University, Kingston, Ontario, 195 p.

**Davis, G.H. and Reynolds, S.J.**

1996: Structural Geology of Rocks and Regions; John Wiley and Sons, Inc., New York, New York, 776 p. (2nd edition).

**Hanmer, S. and Passchier, C.**

1991: Shear-sense indicators: a review; Geological Survey of Canada, Paper 90-17, 72 p.

**Jordan, P.**

1991: Development of asymmetric shale pull-aparts in evaporite shear zones; *Journal of Structural Geology*, v. 13, p. 399–409.



**MacGeehan, P. and Hodgson, C.J.**

1982: Environments of gold mineralization in the Campbell Red Lake and Dickenson mines, Red Lake district, Ontario; *in* Geology of Canadian Gold Deposits; Canadian Institute of Mining and Metallurgy, Special Volume 24, p. 184–207.

**Mathieson, N.A.**

1982: Geology and mineralization in the area of the East South 'C' ore zone, Dickenson mine, Red lake district, northwestern Ontario; M.Sc. thesis, Queen's University, Kingston, Ontario, 155 p.

**Mathieson, N.A. and Hodgson, C.J.**

1984: Alteration, mineralization, and metamorphism in the area of the East South C ore zone, 24th level of the Dickenson mine, Red Lake, northwestern Ontario; Canadian Journal of Earth Sciences, v. 21, p. 35–52.

**Parker, J.R.**

2000: Gold mineralization and wall rock alteration in the Red Lake greenstone belt: a regional perspective; *in* Summary of Field Work and Other Activities, Ontario Geological Survey, Open File Report 6032, p. 22-1–22-28.

**Penczak, R. and Mason, R.**

1997: Metamorphosed Archean epithermal Au-As-Sb-Zn-(Hg) vein mineralization at the Campbell Mine, northwestern Ontario; Economic Geology, v. 92, p. 696–719.

**Ramsay, J.G. and Huber, M.**

1987: Folds and fractures; Volume 2 *in* The Techniques of Modern Structural Geology; Academic Press, London, United Kingdom, p. 457–463.

**Rigg, D. and Helmsteadt, H.**

1981: Relationships between structures and gold mineralization in Campbell Red Lake and Dickenson Mines, Red Lake area, Ontario; Ontario Geological Survey, Miscellaneous Paper 97, p. 111–127.

**Rogers, J.**

1992: The Arthur W White Mine, Red Lake area, Ontario: detailed structural interpretation the key to successful grade control and exploration; Canadian Institute of Mining and Metallurgy, Bulletin 85, no. 957, p. 37–44.

**Sanborn-Barrie, M., Skulski, T., and Parker, J.**

2001: Three hundred million years of tectonic history recorded in the Red Lake greenstone belt, Ontario; Geological Survey of Canada, Current Research 2001-C19.





**Sanborn-Barrie, M., Skulski, T., Parker, J., and Dubé, B.**

2000: Integrated regional analysis of the Red Lake belt and its mineral deposits, western Superior Province, Ontario; Geological Survey of Canada, Current Research 2000C-18, 16 p. (online; <http://www.nrcan.gc.ca/gsc/bookstore>)

**Tarnocai, C., Hattori, K., and Stubens, T.C.**

1998: Metamorphosed Archean epithermal Au-As-Sb-Zn(Hg) vein mineralization at the Campbell Mine, northwestern Ontario - a discussion; *Economic Geology*, v. 96, p. 683–688.

**Zhang, G., Hattori, K., and Cruden, A.**

1997: Structural evolution of auriferous deformation zones at the Campbell Mine, Red lake greenstone belt, Superior province; *Precambrian Research*, v. 84, p. 83–103.

---

Geological Survey of Canada Project 970019

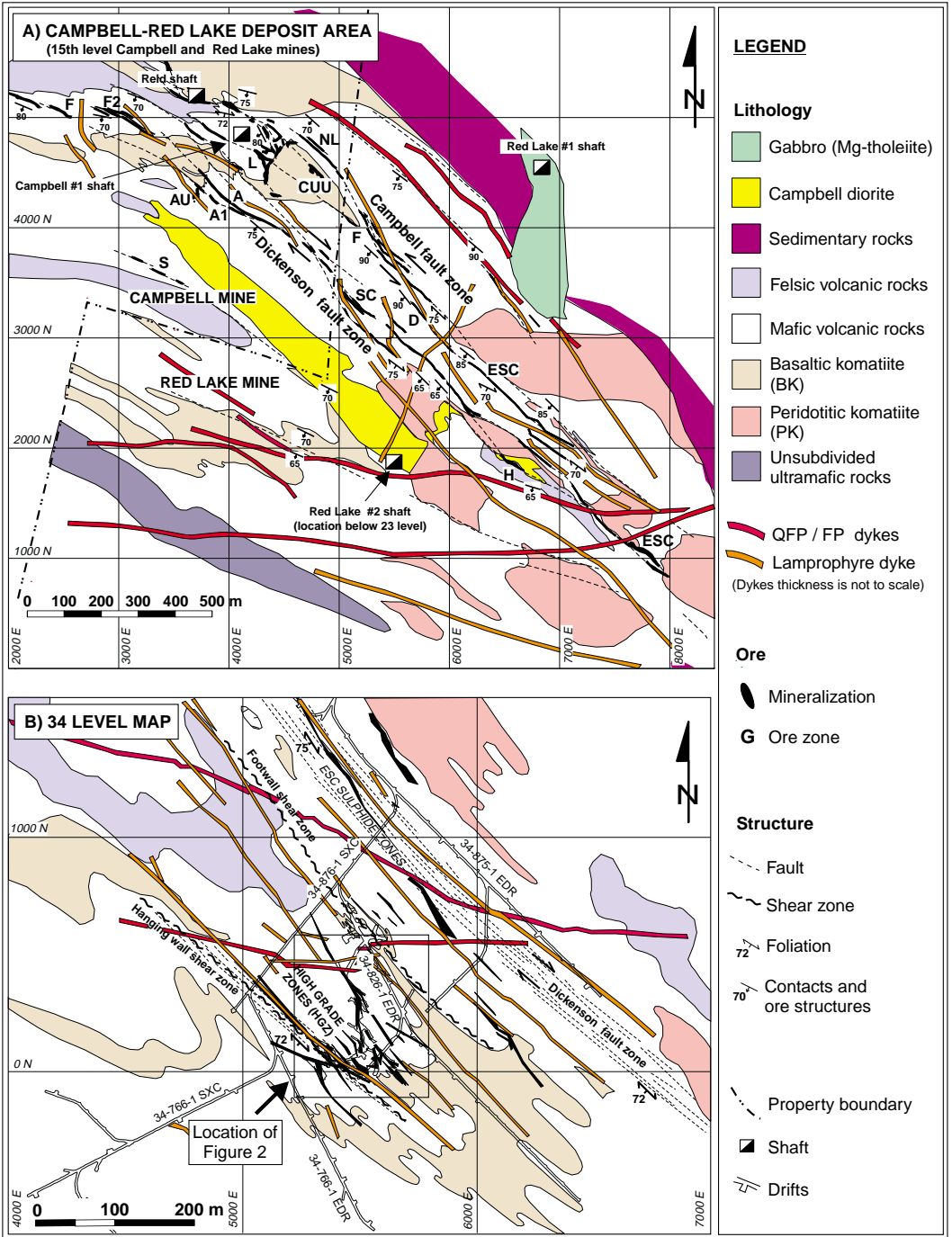


**Figure 1. A)** Geology of the 15th level at the Campbell-Red Lake deposit (*modified from Goldcorp Inc. geological data*). **B)** Geology of level 34, Red Lake mine (*modified from Goldcorp Inc. geological data*). QFP, quartz feldspar porphyry; FP, feldspar porphyry.

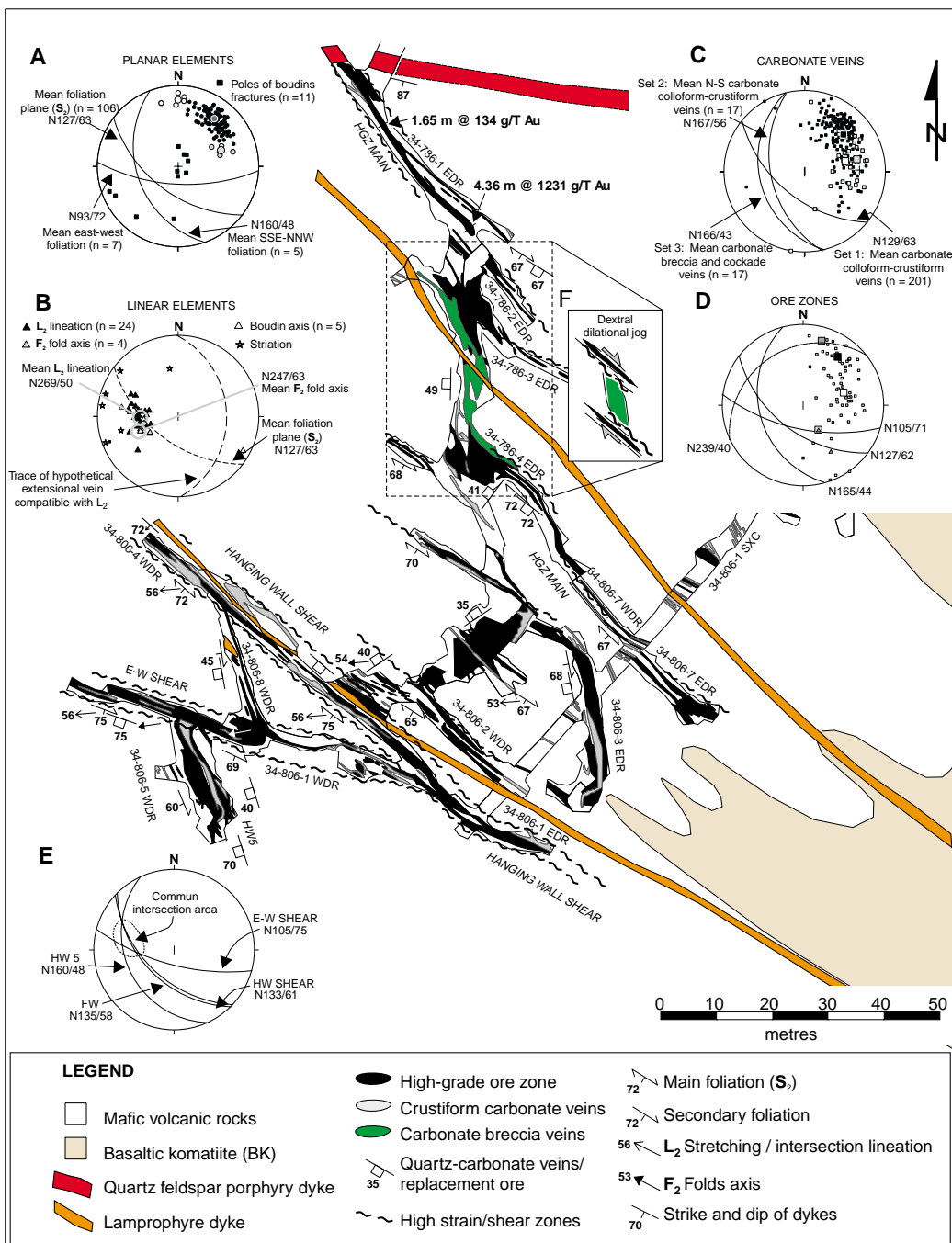


**Figure 2.** Detailed geology of the High Grade zone level 34 at Red Lake mine (modified from Goldcorp Inc. geological data). Stereoplots are equal area projections (lower hemisphere).

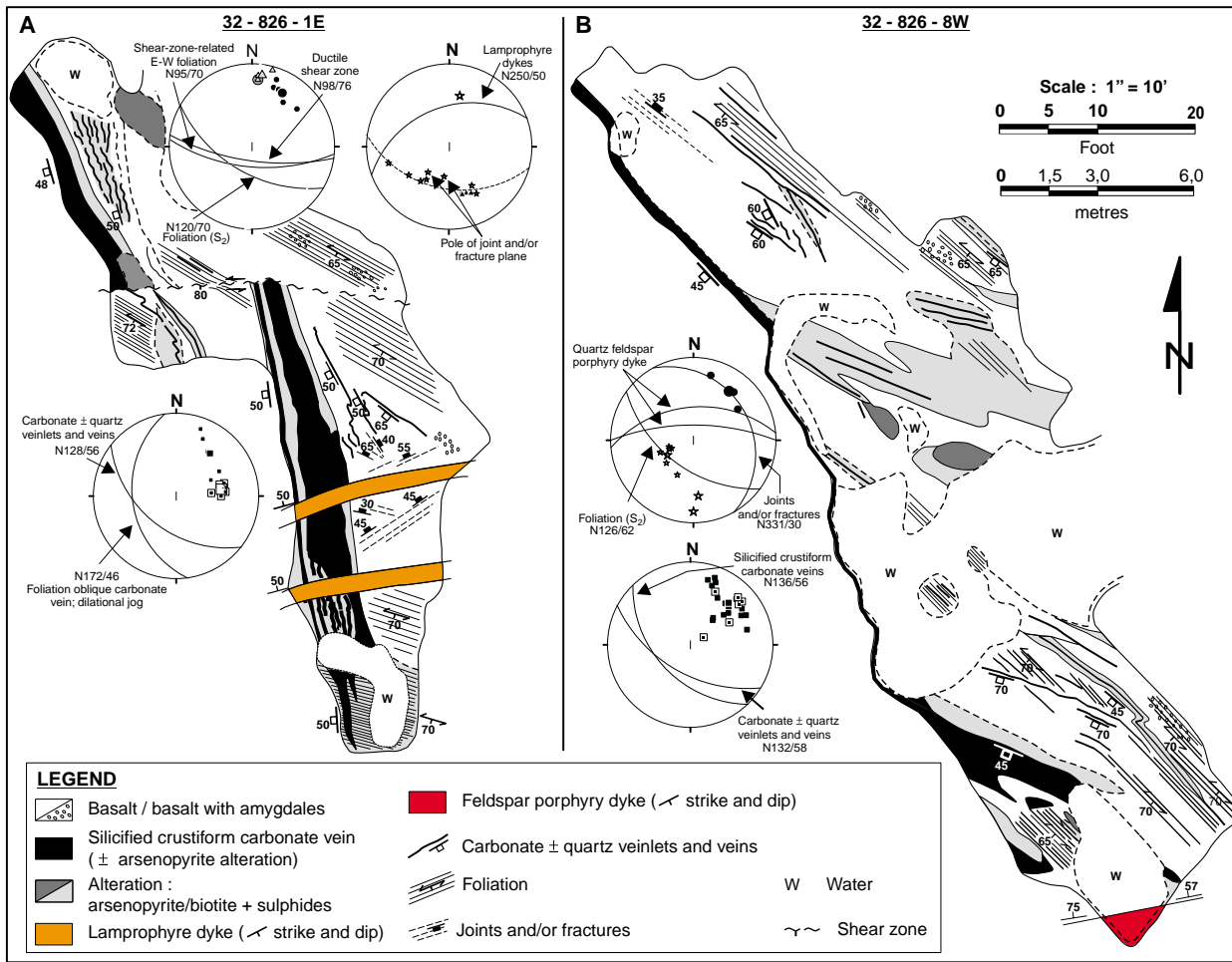


**Figure 3.** Geology floor plan of 32-826-1E and 32-826-8W stopes, level 32. Stereoplots are equal-area projections (lower hemisphere).

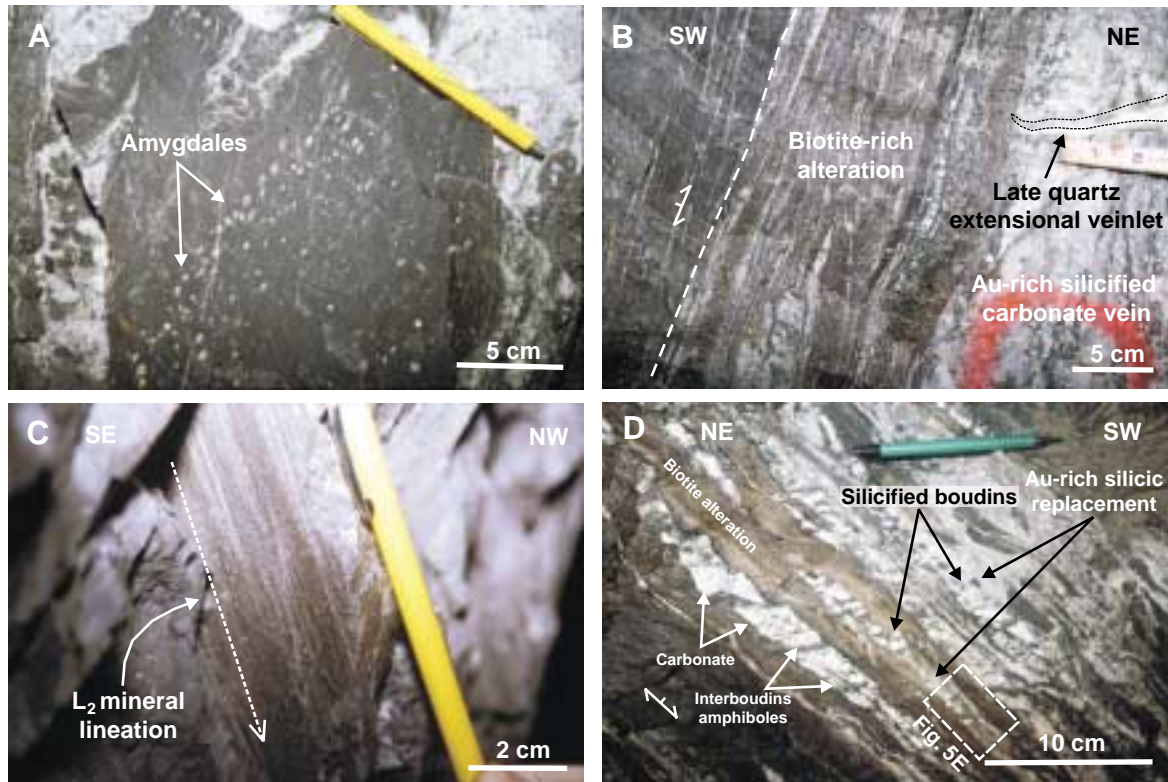


**Figure 4.** A) Weakly deformed amygdales in basalt located in fold nose. B) Section view of foliation-parallel Au-rich silicified carbonate vein in high strain hanging wall shear with strongly foliated biotite alteration. C) Longitudinal view of steeply plunging  $L_2$  stretching lineation. D) Section view of asymmetric boudins deforming extensional carbonate vein replaced by Au-rich quartz, hanging-wall-side-up.

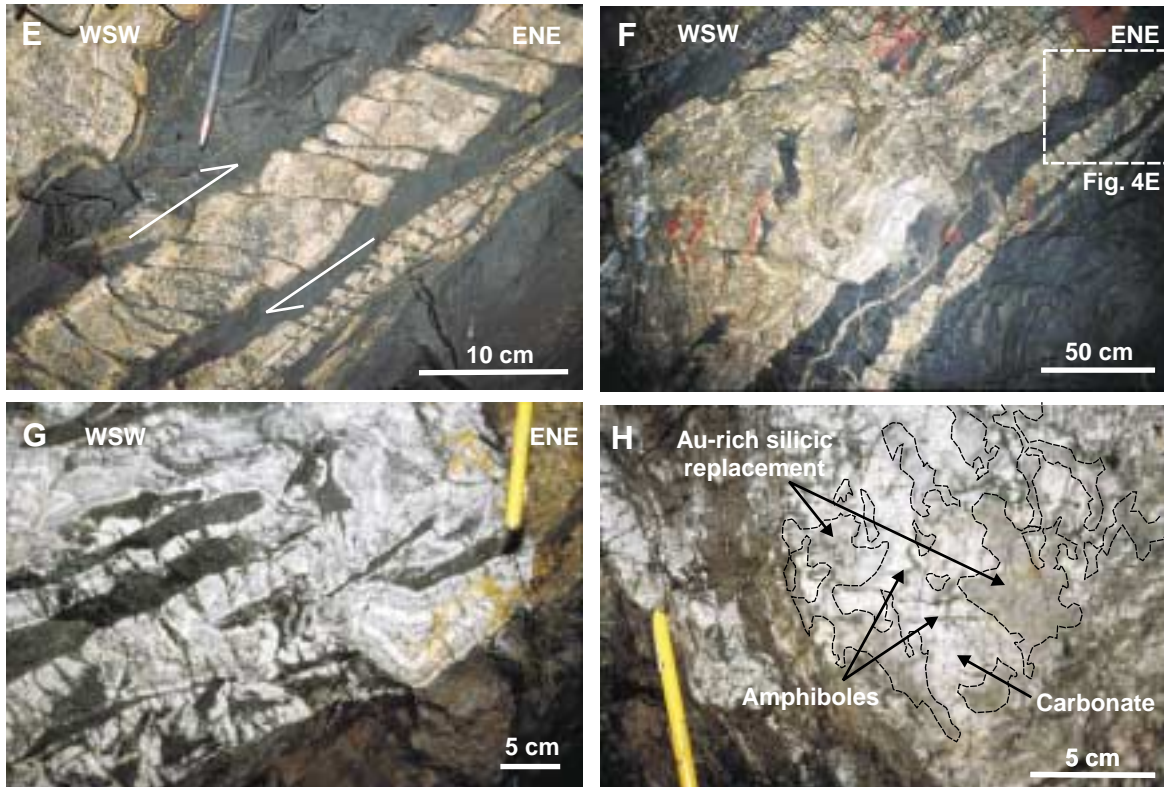


**Figure 4.** **E)** Section view of asymmetric boudins deforming colloform carbonatite vein, hanging-wall-side-up. **F)** Section showing northwest-trending type 3 breccia vein with colloform-cockade breccia texture. **G)** Colloform and cockade textures in carbonatite extensional breccia vein. **H)** Gold-rich quartz replacing carbonatite vein.

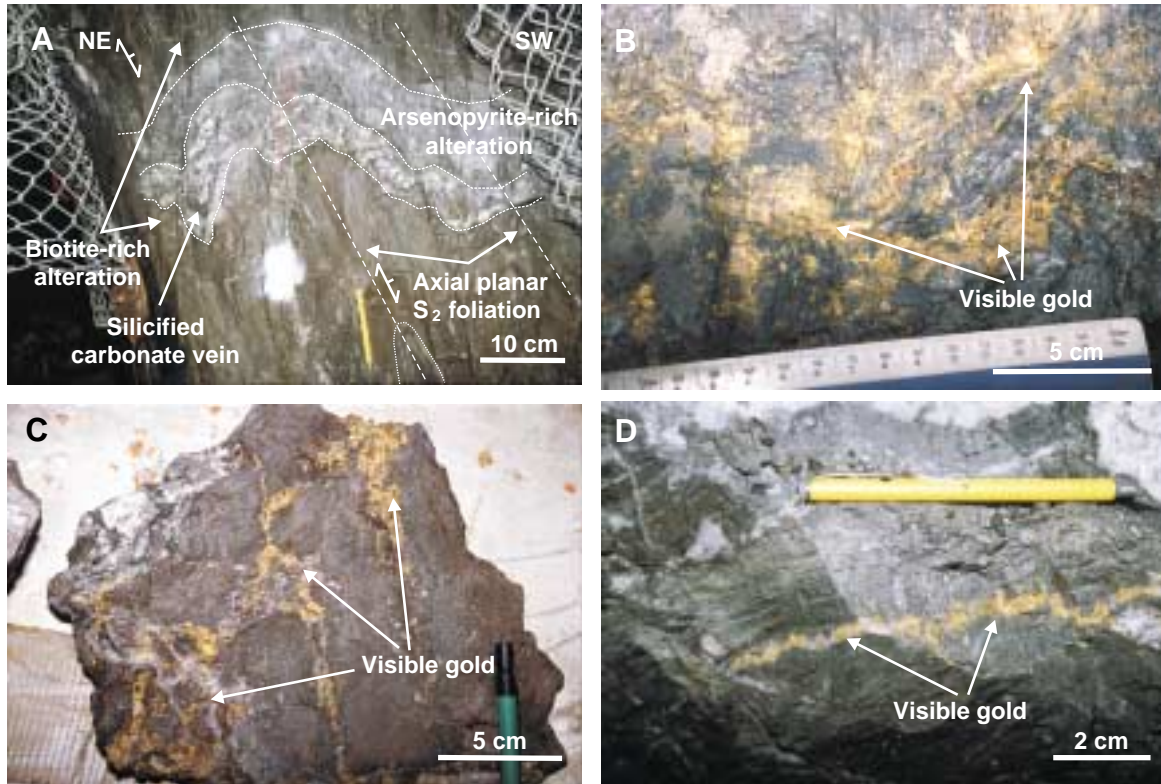


**Figure 5.** A) Shallow-dipping high-grade arsenopyrite-rich silicified carbonate vein and selvages folded by  $F_2$ , section view. B) Visible gold coating late, shallow-dipping fracture. C) Gold veinlets stockwork. D) Extensional carbonate veinlet replaced by quartz containing abundant visible gold and cutting replacement-breccia style ore.

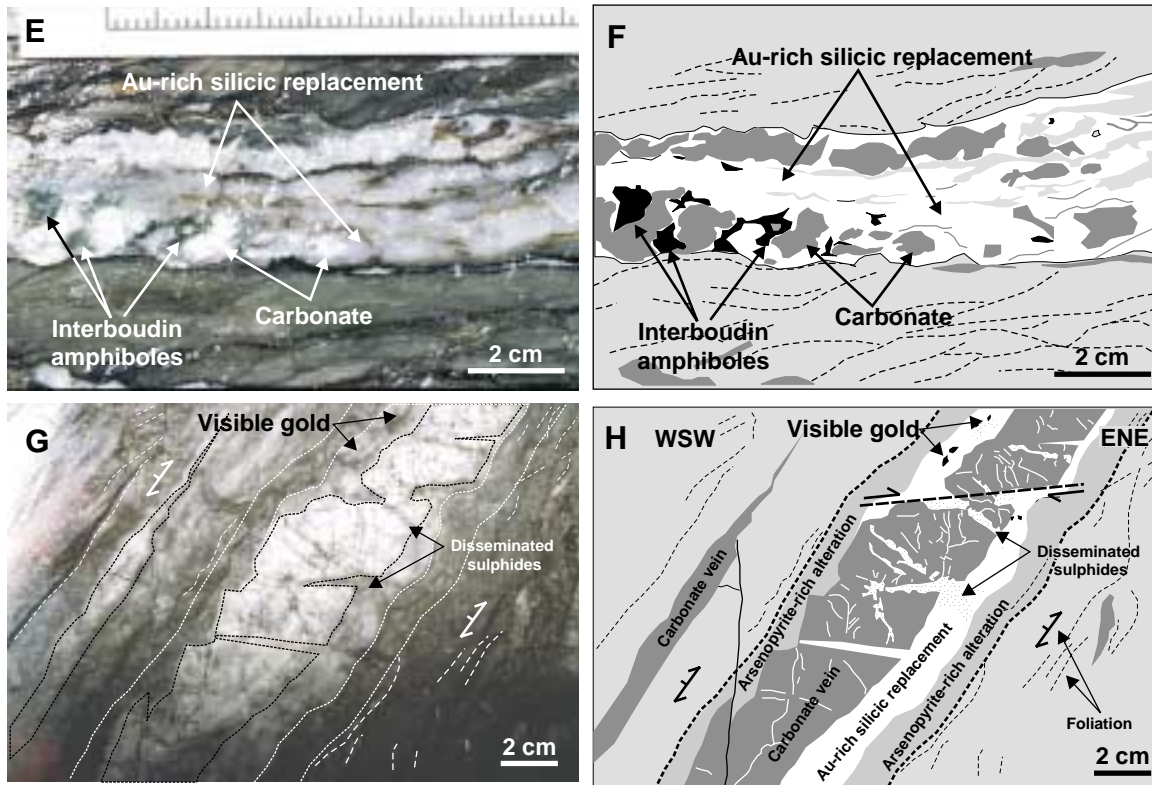


**Figure 5.** E) Gold-rich quartz replacing already boudinaged carbonate vein as well as the amphibole in pull-aparts. F) Drawing of Figure 5E. G) Boudinaged steeply dipping carbonate vein partly replaced by Au-rich silica with quartz filling pull-aparts and both carbonate and quartz being locally cut by subhorizontal shear plane, hanging-wall-side-up, section view. H) Drawing of Figure 5G.



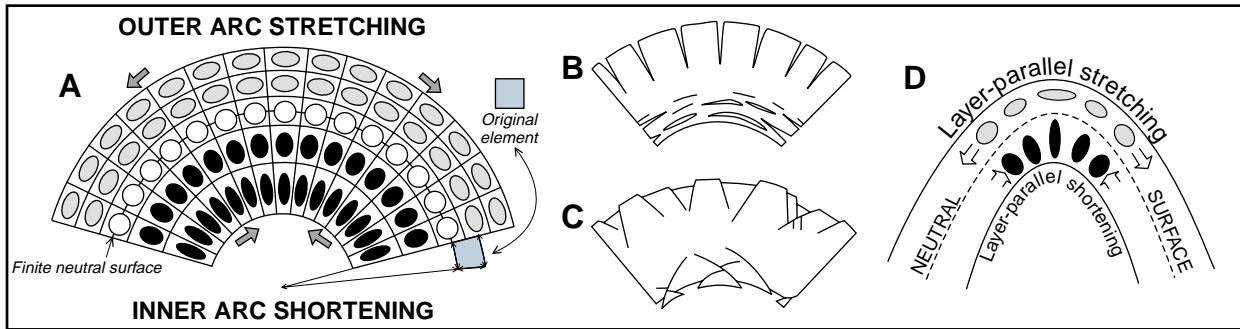


**Figure 6. A)** Geometrical features of fold formed under conditions of tangential longitudinal strain in a competent layer. **B)** Extension fissures. **C)** Conjugate shear faults (after Ramsay and Huber, 1987). **D)** Fold-related layer-parallel stretching and shortening (after Davis and Reynolds, 1996).